FATIGUE OF BRIDGING CERAMICS: UNDERSTANDING CRACK SIZE EFFECTS

J. J. Kruzic, R. M. Cannon, R. O. Ritchie
Department of Materials Science and Engineering, University of California, Berkeley,
and Materials Sciences Division, Lawrence Berkeley National Laboratory, Berkeley, CA 94720 USA

ABSTRACT

Grain bridging is an effective toughening mechanism in non-transforming ceramics; however, it also allows for susceptibility to premature fatigue failure under cyclic loading conditions due to bridge degradation. As with fracture toughness, a crack size dependence on the fatigue properties is expected, specifically at small crack sizes as the bridging zone forms and develops. For ceramics this is especially important since their low inherent toughness dictates that incipient flaws must be quite small (micron scale) to achieve adequate strength. Thus, fatigue properties for flaws on this size scale must be understood for cyclic loading applications. To date, however, the availability of fatigue data exhibiting this crack size dependence has been extremely limited, owing to the difficulty of growing and monitoring very small fatigue cracks in ceramics. Thus, the aim of the present work is to demonstrate and understand crack size effects on the fatigue of bridging ceramics and to create a methodology for reliability predictions under cyclic loading conditions. The material chosen for this study was a commercial alumina (~ 25 μm grain size), which forms large, several millimeter, bridging zones allowing for fatigue behavior to be monitored during bridging zone formation. Furthermore, by deducing and integrating the bridging stress function for a near-threshold steady-state fatigue crack, predictions are made for useful fatigue thresholds over a wide range of crack sizes in the form of a *fatigue threshold R-curve*. Such predictions compare favorably with experimental results for measured fatigue thresholds of short cracks and provide a means for predicting reliability under cyclic loading akin to the methods used for fast fracture.

1. INTRODUCTION

One trade off encountered in making high toughness ceramics has been their susceptibility to cyclic fatigue failure, which is in contrast to ideally brittle ceramics which are considered immune to cyclic fatigue. Fatigue crack growth in ceramics tends to follow the classic Paris law relation:

$$da/dN = C\Delta K^m, \qquad (1)$$

where C is a material specific constant, da/dN is the crack growth rate, and ΔK is the stress intensity range $K_{max} - K_{min}$, where K_{max} and K_{min} are the maximum and minimum stress intensities experienced during the loading cycle, respectively. The Paris law exponent, m, is also material specific and it typically in the range of 15-100 for ceramics. Because of this high stress intensity dependence, propagating fatigue cracks in ceramics will typically grow very quickly to failure. Accordingly, the fatigue threshold, ΔK_{TH}, below which cracks do not propagate under cyclic loading, is considered the most important parameter in the fatigue of ceramics.

Fatigue tests typically done on ceramic materials have utilized cracks with steady-state bridging zones, where bridges are created and destroyed at an equal rate and the size of the zone is

equilibrated at each ΔK value. Crack size effects on the fatigue threshold are ignored in such experiments, and measured fatigue thresholds are non-conservative when compared with smaller cracks with developing, or transient, bridging zones [1]. Because relevant crack sizes in ceramics are several orders of magnitude smaller than those typically tested, the effects of crack size must be addressed if the fatigue threshold is to be used as a design parameter.

The present paper will demonstrate an approach to address crack size effects in fatigue by determining the contribution of bridging in reducing the applied stress intensity at a particular crack size, $K_{br}(\Delta a_f)$, and subtracting it from the steady-state threshold, $\Delta K_{SS,TH}$ to get a crack size dependant threshold, $\Delta K_{TH}(\Delta a_f)$, using:

$$\Delta K_{TH}(\Delta a_f) = \Delta K_{SS,TH} - K_{br}(\Delta a_f), \qquad (2)$$

where Δa_f refers to the fatigue crack extension. This approach allows the construction of a *fatigue threshold R-curve*, which can be used for reliability predictions under cyclic loading conditions and explicitly accounts for crack size effects. The predicted fatigue thresholds based on Eq. 2 will be compared to actual measurements at various crack sizes to verify the methodology.

2. PROCEEDURES

A commercial 99.5% pure alumina (~ 25 µm grain size, Coors AD995) was chosen as a model material due to the large steady-state bridging zones (~2 mm) it exhibits near the fatigue threshold [1]. This large bridging zone length allowed for direct measurements of fatigue thresholds over a range of crack sizes while the bridging zone was being developed. Fatigue-crack growth experiments were conducted on compact tension, C(T), specimens (width, $W \approx 17$ mm, thickness, $B \approx 3$ mm) in general accordance with ASTM standard E647. Complete details of the fatigue-crack growth procedures may be found in Ref. [1], with a brief summary presented below. Fatigue cracks were initiated from straight machined notches (length $a_o \approx 4 - 5$ mm) under cyclic loading conditions (25 Hz. sine wave, load ratio, $R = K_{min}/K_{max} = 0.1$), after which the cracks were grown to a specified length as monitored using back-face strain compliance methods [2]. Notch root radii, ρ, as small as ~15 µm were used for the smallest crack sizes, and data collection did not begin until the fatigue crack extended at least a distance ρ from the notch. In order to measure the fatigue threshold, the applied ΔK was reduced at a roughly constant ΔK-gradient of -0.08 mm^{-1}. Based on previous results [1], this ΔK-gradient was low enough to achieve steady-state bridging zones for cracks with $\Delta a_f > 2$mm in the range of growth rates typically used, i.e., from ~ 10^{-8} to 10^{-10} m/cycle. The fatigue threshold was thus measured as a function of fatigue crack extension, Δa_f, ranging from 60 µm to 7 mm, with the threshold operationally defined as the driving force at which the fatigue crack growth rate, da/dN, is at or below ~10^{-10} m/cycle.

A brief summary of the methods used to determine the bridging stress distribution, $\sigma_{br}(x)$, for a near-threshold steady-state fatigue crack are outlined here; full details may be found in Ref. [1]. Firstly, the fatigue crack was grown for more than 2 mm, i.e., through the entire bridging zone length, near the fatigue threshold ($da/dN < 7 \times 10^{-10}$ m/cycle). The length of the bridging zone, L, was measured using multi-cutting compliance methods [1,3], whereby the crack wake was incrementally cut out using a diamond saw while making compliance measurements after each incremental cut. By noting the notch length where the compliance began to increase, a roughly L = 2 mm near-threshold bridging zone length was determined. Additionally, the shape of the bridging stress distribution, normalized by the maximum bridging stress, σ_{max}, was determined using [3]:

$$\frac{\sigma_{\mathrm{br}}(x)}{\sigma_{\max}} = -\frac{C^2(a)C_{\mathrm{u}}'(x)}{C'(a)C_{\mathrm{u}}^2(x)}$$ (3)

where $C(a)$ is the traction free compliance, $C_{\mathrm{u}}(x)$ is the observed compliance after cutting to the position x measured from the load line, and $C'(z) = \mathrm{d}C(z)/\mathrm{d}z$.

In order to deduce the value of $\sigma_{\max}$, the crack opening displacements, $u_{\mathrm{tot}}(x)$, were measured in a field emission scanning electron microscope (FESEM) with the sample loaded to $K = 3.0$ MPa√m, which was roughly 10 – 20% lower than the maximum stress intensity at the steady-state fatigue threshold. The crack opening displacements and bridging stress distribution are related through the double integral equation [4]:

$$\frac{1}{E'}\int\limits_0^a \int\limits_{\max(x,x')}^a h(a',x)h(a',x')\sigma_{\mathrm{br}}(x')da'dx' = u_{\mathrm{tot}} - u_{\mathrm{app}},$$ (4)

where E' is Young's modulus (E in plane stress, $E/(1\text{-}v^2)$ in plane strain, where v is Poisson's ratio) and the weight function, h, is geometry specific and for the C(T) specimen may be found in ref. [5]. Also used in Eq. 4 are the displacements due to the applied loading, u_{app}, for an unbridged crack at a given applied stress intensity, K_{app}, which may be calculated as [6]:

$$u_{\mathrm{app}} = \frac{1}{E'}\int\limits_x^a K_{\mathrm{app}}(a')h(a',x)da' \ .$$ (5)

Combining the normalized bridging stress distribution from Eq. 3 with Eqs. 4-5 allows a value for $\sigma_{\max}$ to be obtained, which was determined to be that which gave a crack opening profile nearest that measured experimentally, as determined by the least squares method.

The methods used in the present study to predict fatigue thresholds as a function of crack length, i.e., a fatigue threshold R-curve, are based on those used to predict classical fracture toughness R-curves [4,7-9]. Specifically, the toughening contribution of bridging, K_{br}, is deduced by integrating the bridging stress distribution, in this case using the weight function approach [10]:

$$K_{\mathrm{br}} = \int\limits_0^a h(x,a)\sigma_{\mathrm{br}}(a)dx$$ (6)

For cracks were $\Delta a_{\mathrm{f}} > L$, integrating Eq. 6 gives the steady-state bridging contribution, $K_{\mathrm{SS,br}}$, which is insensitive to crack length, while for cracks where $\Delta a_{\mathrm{f}} < L$ the transient bridging contributions may be determined which exist during the development of the bridging zone. In the present case, σ_{br} represents the (nearly) fully degraded bridging stress distribution for a crack at the fatigue threshold, and accordingly through the use of Eq. 6, the near-threshold bridging contributions for any crack length may be deduced

3. RESULTS AND DISCUSSION

Fig. 1 shows typical fatigue crack growth results for AD995 alumina in the form of da/dN-ΔK curves for a range of different crack sizes. From Fig. 1 it is apparent that there is a distinct crack size effect on the fatigue threshold; indeed, ΔK_{TH} values were roughly 50% lower for cracks where

$\Delta a_f = 60$ μm when compared to steady-state cracks with $\Delta a_f > L = 2$ mm. Because typical fatigue thresholds are measured on nominally steady-state cracks many millimeters in length, Fig. 1 illustrates the necessity of considering the fatigue properties for realistic flaw sizes in ceramics, i.e., 10s - 100s of microns. One approach to this problem is the use a fatigue threshold R-curve, shown in Fig. 2. The data points in Fig. 2 represent measured fatigue thresholds plotted as a function of fatigue crack extension, Δa_f. For crack sizes where $\Delta a_f > L$, these fatigue thresholds correspond to steady-state fatigue cracks, where bridges are exhausted and created at an equal rate and the nature of the bridging zone uniquely corresponds to the applied ΔK level. Such steady-state fatigue thresholds should not be history or size dependent, provided steady-state conditions are always maintained while approaching the fatigue threshold. For transient cracks with $\Delta a_f < L$, the measured fatigue thresholds are certainly size dependent; however, it is presumed for most samples that any history dependence on the thresholds should be minimal for cracks grown under identical conditions to the steady-state cracks, where history dependence was not observed for growth rates in the 10^{-10} - 10^{-8} m/cycle range [1]. In some cases, however, initial growth rates were higher than 10^{-8} m/cycle and the measured threshold may have been elevated by history effects if bridges which formed at the higher growth rates had not degraded sufficiently at the measured fatigue threshold. Thus, a conservative assessment of the data for $\Delta a_f < L$ would be as upper bounds to the lowest achievable fatigue threshold at each crack size.
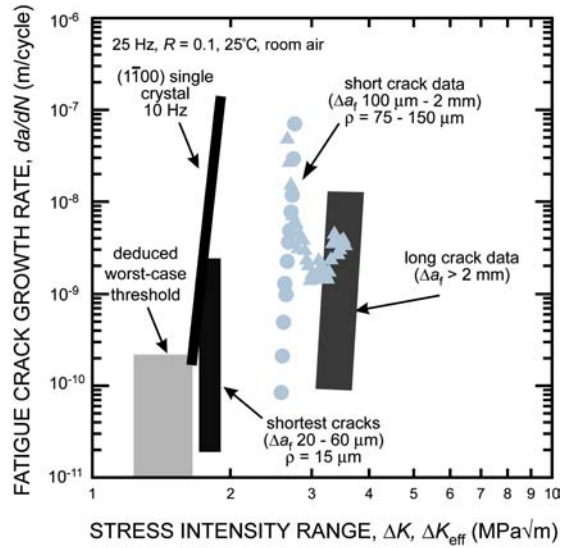

Figure 1: Fatigue crack growth data for AD995 alumina at various crack sizes. Additionally shown are data for sapphire from Ref. [11] and the deduced "worst-case" threshold from Fig. 2.

Fig. 3 shows the bridging stress distribution for a near-threshold steady-state fatigue crack in this alumina deduced using Eqs. 3-5. Since the crack was grown near the fatigue threshold ($da/dN < 7 \times 10^{-10}$ m/cycle) through the entire bridging zone, this is considered to be a good estimate of the fully degraded bridging stress distribution for a near-threshold fatigue crack. Thus, applying Eq. 6, the bridging contribution, K_{br}, to the measured fatigue threshold may be predicted for any crack size and accordingly the fatigue threshold R-curve may be predicted using Eq. 2. This prediction is plotted in Fig. 2 along with the measured data. Additionally, the "worst-case" fatigue threshold, corresponding to the initial point on the fatigue threshold R-curve in Fig. 2, is plotted in Fig. 1.

Note that no cracks grew below the deduced worst case threshold, and additionally this threshold fell below the driving forces expected for cracking in sapphire [11], which is consistent with the intergranular crack path which is observed.
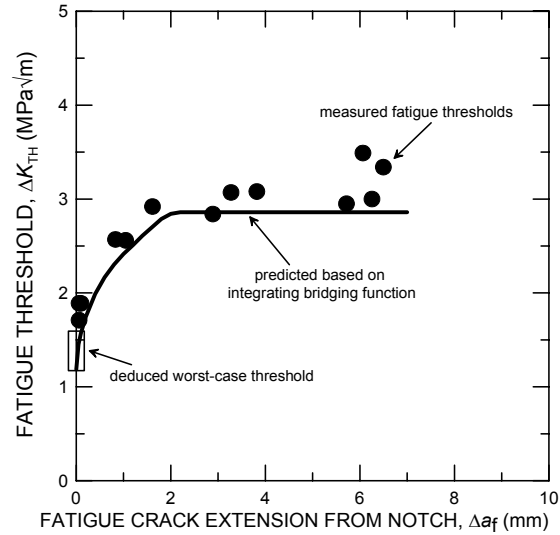

Figure 2: The fatigue threshold R-curve for AD995 alumina. Individual data points represent experimentally measured thresholds, while the line gives the predictions based on Eqs. 2 & 6.
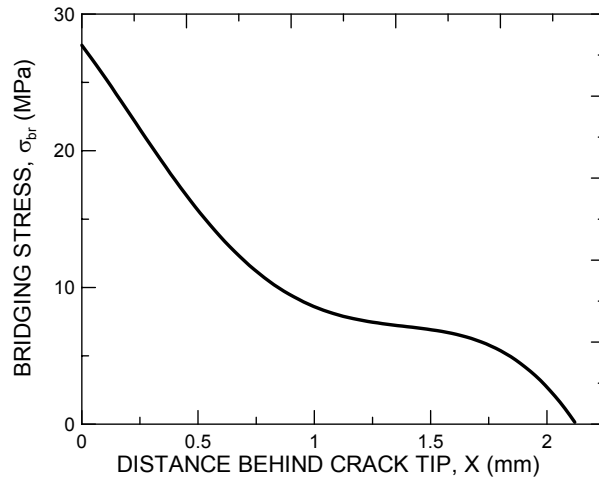

Figure 3: The bridging stress distribution for a near-threshold steady-state fatigue crack in AD995 alumina.

It is apparent in Fig. 2 that the predicted fatigue threshold R-curve provides a lower bound below which cracks were not observed to propagate over the full range of transient crack sizes up to the steady-state regime. Furthermore, such predictions were made using only fatigue results for long, steady-state fatigue cracks without the need for direct short crack experiments. This is desirable since direct short crack testing over relevant size scales is often prohibitively difficult for

many structural ceramics of interest, e.g., self-reinforced Si_3N_4 and SiC; although, it should be noted that other methods for determining the bridging stress distribution may be required for such materials, which have bridging zones only 10's to 100's of microns long. Furthermore, such fatigue threshold R-curves may be used to make reliability predictions in bridging ceramics under cyclic loading conditions, similar to how fracture toughness R-curves can be used to predict reliability under monotonic loading by relating internal flaw distributions to failure stress levels.

4. CONCLUSIONS

Based on an experimental study of the fatigue behavior of a bridging 99.5 % pure commercial alumina, it has been shown that crack size effects are an important consideration when determining fatigue thresholds in bridging ceramics. Furthermore, crack size effects may be expressed via a *fatigue threshold R-curve*, which can: 1) be predicted from the bridging stress distribution, and 2) be utilized for reliability predictions under cyclic loading conditions, analogous to a fracture toughness R-curve for monotonic loading conditions.

ACKNOWLEDGEMENTS

REFERENCES

1.   Kruzic, J.J., Cannon, R.M., and Ritchie, R.O., "Crack size effects on cyclic and monotonic crack growth in polycrystalline alumina: Quantification of the role of grain bridging." *J. Am. Ceram. Soc.*, **87**(1): 93-103, 2004.
2.   Deans, W.F. and Richards, C.E., "A simple and sensitive method of monitoring crack and load in compact fracture mechanics specimens using strain gages." *J. Test. Eval.*, **7**(3): 147-154, 1979.
3.   Wittmann, F.H. and Hu, X., "Fracture process zone in cementitious materials." *Int. J. Fract.*, **51**(1): 3-18, 1991.
4.   Fett, T., Munz, D., Seidel, J., Stech, M., and Rödel, J., "Correlation between long and short crack R-curves in alumina using the crack opening displacement and fracture mechanical weight function approach." *J. Am. Ceram. Soc.*, **79**(5): 1189-1196, 1996.
5.   Fett, T. and Munz, D., *Stress Intensity Factors and Weight Functions*. Southampton, UK: Computational Mechanics Publications, pp. 408, 1997.
6.   Fett, T., Mattheck, C., and Munz, D., "On the calculation of crack opening displacement from the stress intensity factor." *Eng. Fract. Mech.*, **27**: 697-715, 1987.
7.   Fett, T., Munz, D., Dai, X., and White, K.W., "Bridging stress relation from a combined evaluation of the *R*-curve and post-fracture tensile tests." *Int. J. Fract.*, **104**: 375-385, 2000.
8.   Lawn, B., *Fracture of Brittle Solids*. 2nd ed. Cambridge Solid State Science Series, ed. E.A. Davis and I.M. Ward. Cambridge, UK: Cambridge University Press, pp. 378, 1993.
9.   Mai, Y.-W. and Lawn, B.R., "Crack-interface grain bridging as a fracture resistance mechanism in ceramics: II, Theoretical fracture mechanics model." *J. Am. Ceram. Soc.*, **70**(4): 289-294, 1987.
10.   Bueckner, H.F., "A novel principle for the computation of stress intensity factors." *Z. Angew. Math. Mech.*, **50**(9): 529-546, 1970.
11.   Asoo, B., McNaney, J.M., Mitamura, Y., and Ritchie, R.O., "Cyclic fatigue-crack propagation in sapphire in air and simulated physiological environments." *J. Biomed. Mater. Res.*, **52**: 488-491, 2000.